Production of high-spin isomers in proton induced reactions at 100–500 MeV on ^{181}Ta

B. L. Zhuikov,* M. V. Mebel,† V. M. Kokhanyuk, and A. S. Iljinov
Institute for Nuclear Research of the Russian Academy of Sciences, 117312 Moscow, Russia

A. Yu. Zyuzin and J. S. Vincent
TRIUMF, 4004 Wesbrook Mall, Vancouver, British Columbia, Canada V6T 2A3
(Received 22 September 2002; revised manuscript received 27 March 2003; published 25 November 2003)

Cross sections for production of a broad variety of high-spin isomers, i.e., ^{177}Hf^{m2}(37/2$^-$), ^{179}Hf^{m2}(25/2$^-$), ^{177}Lu^m(23/2$^-$), ^{180}Hf^m(8$^-$), and ^{178}Ta^m(7$^-$) from ^{181}Ta targets irradiated with 100, 145, 200, 350, and 500 MeV protons have been measured by off-line γ-spectroscopy. A radiochemical procedure was used to achieve high sensitivity. Isomer ratios in products ranging down to 10^{-3} were based on experimentally measured and theoretically calculated cross sections. It was demonstrated that the isomer ratio does not depend essentially on proton energy in the given range. Regularities in formation of isomeric states in different nuclear reactions are discussed.

DOI: 10.1103/PhysRevC.68.054611 PACS number(s): 13.75.−n, 24.10.−i, 25.60.Dz, 27.70.+q

I. INTRODUCTION

The phenomenon of high-spin isomer formation is an important problem associated with the transfer of a large amount of angular momentum in nuclear reactions. There are numerous experimental data investigating this process with heavy ions. There are also results reported for the reactions induced by π^- [1–4]. A theoretical interpretation of the experimental results and nuclear mechanism has been suggested [5–7]. Till date, only a few separate results of isomeric state formation by protons have been published (e.g., the production of ^{177}Lu^m at 100 and 500 MeV measured at LAMPF [3]). The objective of our experiments was to investigate general regularities of this phenomenon for proton induced reactions. ^{181}Ta targets were bombarded over a wide energy range (100–500 MeV) to produce a broad variety of isomers, including ^{177}Hf^{m2} with the highest spin value 37/2 $\hbar$. The interpretation of results may be important for the understanding of the mechanism of intermediate-energy particle interaction with nuclei.

II. EXPERIMENT AND RESULTS

The experiments were performed at the TRIUMF cyclotron and the LINAC of the Institute for Nuclear Research. Targets made of metallic tantalum (foils ~0.1 mm thick) were irradiated by protons with energies of 100, 145, 200, 350, and 500 MeV. Proton energy loss due to degrading materials before the target (calculated from data given in Ref. [8]) was always less then 15 MeV. The foil stack was thin enough, so that activation from secondary pions and neutrons could be neglected. The uncertainty in the reported proton energies due to the use of the stack foil technique and target holder design was estimated as ±2 MeV or less. The average proton current varied from 0.5 to 10 μA in different irradiations. Irradiation time was varied from several minutes to several hours for long-lived isotopes. Targets were removed quickly with the help of a rabbit system for γ-spectroscopy measurement and/or radiochemical processing began a few minutes after the irradiation when necessary.

To measure the total charge of protons, monitor foils of aluminum, copper, tungsten and gold were inserted into the foil stack. The cross sections for monitor reactions Al $\rightarrow$ ^{22}Na, Cu $\rightarrow$ ^{62}Zn, W $\rightarrow$ ^{181}Re, and Au $\rightarrow$ ^{192}Hg were taken from a handbook [9].

Since a wide range of isotopes of various chemical elements was produced in these experiments, it was necessary to perform chemical separation of the products so that the γ-lines could be analyzed unambiguously and with high sensitivity. Radiochemical processing was based on the formation of fluoride and sulphate complexes and their separation using anion exchange resin. The detailed procedure is as follows.

(i) Metallic tantalum was dissolved in 10*M* HF with a few drops of HNO_3.

(ii) The solution was evaporated and transferred to 1*M* HF.

(iii) This solution was passed through an ion exchange column of DOWEX-1×8 to absorb Hf, Ta, W, and Lu. Other lanthanides were not absorbed and passed through the column (fraction I).

(iv) Lu was eluted by the solution 0.1*M* H_2SO_4 +2%H_2O_2 (fraction II).

(v) Hf was eluted by the solution 0.4*M* H_2SO_4 +2%H_2O_2 (fraction III).

(vi) Ta and W were eluted by the solution 2*M* H_2SO_4 +2%H_2O_2 (fraction IV).

(vii) The remaining tungsten was eluted by the solution 9*M* HCl+3*M* HF (fraction V).

Each eluate fraction was evaporated to make the final sample for γ-spectroscopy measurements. The effectiveness of chemical separation is demonstrated by Table I.

The time period from the end of bombardment up to the beginning of the chemical processing was few minutes or

*Electronic address: bz@inr.troitsk.ru
†Electronic address: mebel@cpc.inr.ac.ru

TABLE I. Distribution of chemical elements in various fractions of the radiochemical processing (%).

Chemical element	Eluate fraction I	II	III	IV	V
Lanthanides	98	2			
Lu	15	85			
Hf		0.3	99.7		
Ta			6	93	1
W			1	86	13

more, and about 2.5 h to the beginning of measurements of Hf fraction. Measurements of the shortest-lived nuclides were performed without radiochemical separation.

The γ-spectroscopy measurements used Ge detectors with energy resolution of 0.8 keV for 122-keV γ-line of ^{57}Co. The spectra contained several hundred γ-lines even after the chemical separation. Nuclear data tables [10] were used for identification of γ-lines. A computer code GXL [11] was used to analyze the data. It effectively resolves γ-lines with comparable intensity and energy difference of 0.2 keV.

Each cross section was evaluated using the isotope yield from the sample containing the most abundant chemical fraction as shown in Table I. This fraction produced the most intense and unambiguous γ-lines for statistical analysis. Calculation of the cross section took into account the following factors: yields from less abundant chemical fractions, decay during irradiation and chemical processing, detector efficiency, and beam monitoring. Statistical uncertainties in chemical yield and γ ray counts were added in quadrature to the systematic errors noted above to arrive at the cross section uncertainty (1σ criteria) given in Tables II and III.

Identification of isomers with the highest spin was the most difficult problem. To identify ^{177}Hf^{m2} ($37/2^-$), only the most intense γ-line with energy of 277.3 keV provided a reliable detection of the radionuclide (Fig. 1). Other lines of this isomer (although the computer code found them in the spectrum) were uncertain because of interference from contaminant γ-lines. The 208.4-keV γ-line, as well as those at 418.5 and 413.7 keV, was used for identification of Lu^m ($23/2^-$), and the 453.7-keV γ-line for identification of ^{179}Hf^{m2} ($25/2^-$). The production cross sections for isomers ^{180}Hf^m (8^-) and ^{178}Ta^m (7^-) were also measured.

It was not possible to determine the cross sections for ground states of the same nuclides experimentally in the most cases. For instance, all the Hf isotopes are stable while ^{178}Ta is too short lived. We were able to measure only the ground state cross section for ^{177}Lu at 100 MeV. Large amounts of other radionuclides made the measurements of ^{177}Lu at higher proton energies not reliable. However a number of other radionuclides have been measured (Table III) to validate the use of our reaction calculations.

III. DISCUSSION

The formation of high-spin isomeric states in nuclear reactions with protons was discussed earlier in the framework of the standard cascade nucleon emission mechanism [5]. According to this consideration the incident proton generates a cascade of sequential nucleon-nucleon collisions, and high-energy particles escape from the nucleus. There may also be a contribution of the competitive process of precompound cluster emission [16]. The angular momentum of the final nucleus is a result of the transfer of orbital angular momentum from the incident proton plus its coupling with the spin of the target nucleus. Additional angular momentum may be imparted by the outgoing proton or by an α cluster impacted at the nuclear periphery. The existence of a preformed cluster in the nucleus is suggested by the small value of binding energy for this cluster of nucleons (−1.5 MeV for an α particle in the case of ^{181}Ta).

A. Cross sections

Systematics for isomeric state production behavior are given in Fig. 2. The dependence of the cross section on proton energy in the case of formation of ^{178}Ta^m (7^-) in $(p, p3n)$ reaction is quite typical for a reaction with neutron evaporation. The cross section decreases slowly with increasing energy because of competition with the evaporation process for more neutrons. The general magnitude of the cross section is relatively high in this case (Fig. 2). Evidently this process of

TABLE II. Production cross sections σ^m (mb) for high-spin isomers from measurements with 100, 145, 200, 350, and 500 MeV proton bombardment of ^{181}Ta target.

Isomer ($spin^\pi$) $T_{1/2}$	Reaction	Proton energy (MeV) 100	145	200	350	500
^{178}Ta^m (7^-) 2.5 h	^{181}Ta$(p, p3n)$	34.2±2.5	25±2	21.7±2.0	17.4±1.2	13.1±1.5
^{180}Hf^m (8^-) 5.5 h	^{181}Ta$(p, 2p)$	0.44±0.13		1.17±0.09	1.60±0.11	1.71±0.2
^{177}Lu^m ($23/2^-$) 160 d	^{181}Ta$(p, 3p2n)$	0.022±0.002		0.040±0.013	0.068±0.008	0.11±0.03
^{179}Hf^{m2} ($25/2^-$) 25 h	^{181}Ta$(p, 2pn)$	0.42±0.04		0.44±0.04	0.39±0.03	0.41±0.03
^{177}Hf^{m2} ($37/2^-$) 51 m	^{181}Ta$(p, 2p3n)$	0.038±0.010		$<$0.085	0.036±0.004	0.05±0.01

TABLE III. Experimental and calculated cross sections (mb) values in proton interaction with ^{181}Ta. CEF [12–14], ALICE–HMS-ALICE code [15].

Nuclide	Reaction	Proton energy (MeV)					Average
$T_{1/2}$	Code	100	145	200	350	500	$\sigma_{theor}/\sigma_{expt}$
^{175}Hf (cum.)	^{181}Ta(p, 2p5n)	175±30	130±30	101±10	50±3	34±6	
70 d	CEF	223.5	136.2	106.4	78.6	60.6	1.35±0.32
	ALICE	198.8	146.5	119.1	79.8	64.8	1.39±0.35
^{172}Hf (cum.)	^{181}Ta(p, 2p8n)	32±5	107±60	96±8	40±3	19±2	
1.9 yr	CEF	27.1	104.4	78.8	57.5	46.5	1.31±0.69
	ALICE	179.8	132.3	103.5	70.9	55.4	2.52±1.87
^{170}Hf (cum.)	^{181}Ta(p, 2p10n)	13.6±2	58±7	64.6±7	59±6	43±5	
16 h	CEF	5.4	30.9	45.6	35.5	30.0	0.59±0.13
	ALICE	13.4	128.8	80.9	56.1	45.1	1.29±0.53
^{171}Lu (cum.)	^{181}Ta(p, 3p8n)	24±2	65±5	56±5	68±7	44±4	
8.2 d	CEF	57.5	88.6	84.4	65.5	56.6	1.50±0.54
	ALICE	9.2	122.9	89.3	64.2	53.5	1.21±0.58
^{169}Lu (cum.)	^{181}Ta(p, 3p10n)	1.1±0.2	44±15	47±7	37±4	37±5	
30 h	CEF	1.1	39.9	57.3	46.9	44.4	1.12±0.16
	ALICE	2.8	74.1	67.8	52.5	43.9	1.66±0.53
^{167}Hf (cum.)	^{181}Ta(p, 3p12n)	0.1		14±3	40±2	37±5	
52 m	CEF	0.0	11.5	26.3	29.0	29.0	1.13±0.65
	ALICE	0.0	12.8	50.2	37.6	33.3	1.81±1.54
^{177}W(indep.)	^{181}Ta(p, p5n)	62±6	34±5	12±3	7.5±1.4	7.3±2	
23 h	CEF	57.5	33.3	24.5	15.7	9.9	1.48±0.56
	ALICE	71.8	44.6	31.0	14.7	8.5	1.64±0.62

excitation at a relatively low angular momentum is possible for a large fraction of nuclear matter. In our experiments, after the outgoing particle transfers about $M = 1.5\hbar \sin(\theta)\sqrt{E_p}$ units of angular momentum to the Ta nuclei and the struck nucleon is captured, a heated residual nucleus remains (θ denotes emission angle). This excited nucleus subsequently evaporates three neutrons with little effect on the angular momentum distribution.

The process of ^{180}Hf^m (8^-) formation by (p, 2p) reaction is different. The (p, 2p) reaction occurs when the proton partner escapes without further interaction. The cross section is one to two orders of magnitude lower than in the previous case, though the excited spin is almost the same. This may be explained as the first incident proton generating from a second proton only at the periphery of the nucleus. Otherwise, in the deep-inelastic process the second proton will be involved in an intranuclear cascade interaction through differ-

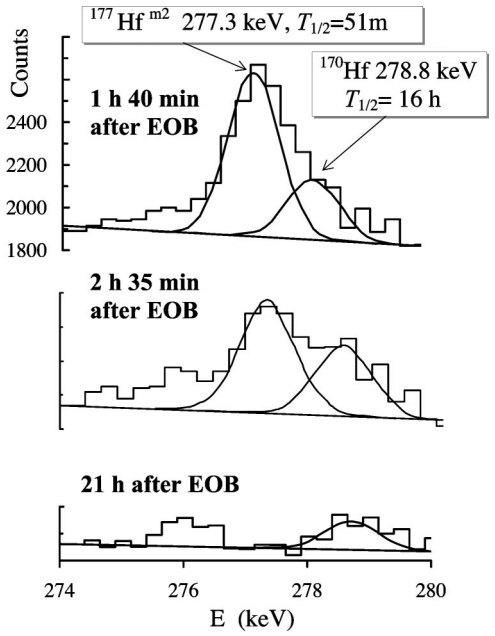

FIG. 1. γ-spectrum of analytical line of ^{177}Hf^{m2} (spin $37/2^-$) after chemical separation. Data for different decay periods after the end of bombardment (EOB) by 100-MeV protons are shown.

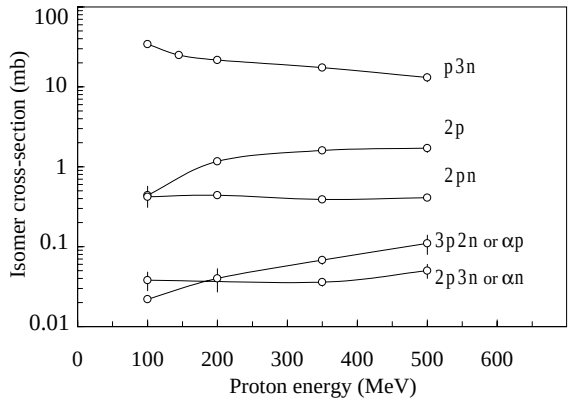

FIG. 2. The experimental results of this work for isomer production cross section.

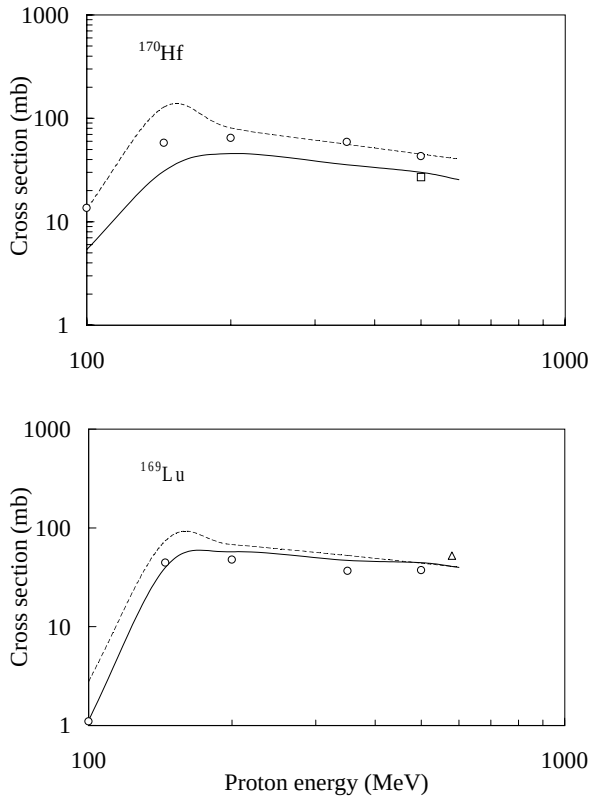

FIG. 3. Excitation function for the ^{181}Ta$(p, 2p10n)$ ^{170}Hf (top panel) and ^{181}Ta$(p, 3p10n)$ ^{169}Lu (bottom panel) reactions. The experimental result of this work (O) is compared with two theoretical predictions: CEF (solid curve) and ALICE (dashed curve) codes; (□) Asano *et al.* [17], (△) Neidhart *et al.* [18].

ent reaction channels. The energy dependence also differs from the $(p, p3n)$ reaction: the cross section increases by a factor of 4–5 with the energy increase from 100 to 500 MeV (Fig. 2). This may be explained by a decrease of the nucleon-nucleon interaction when the energy of the second struck proton correlates with the initial proton energy. Nucleon-nucleon interaction and involvement of the second proton in different reaction channels should decrease with increasing energy. The isomer ratio (see below) is much lower for $(p, 2p)$ than for $(p, p3n)$, resulting in almost the same spin. The emission of the second outgoing proton compensates partly for the angular momentum otherwise transferred by the first proton emission.

The formation of ^{177}Lu^m $(23/2^-)$ may be interpreted as the $(p, 3p2n)$ reaction or $(p, \alpha p)$ reaction. Similarly the cross section increase with proton energy, as in the $(p, 2p)$ reaction (Fig. 2), indicates, indirectly, that the emission of an α particle is more likely. The much lower $(p, \alpha\, p)$ cross section than in the $(p, 2p)$ case is understandable. It is less probable for the incident proton to find a preformed α cluster than a nucleus at the nuclear periphery and to consequently excite the nucleus to such a high spin as 23/2.

In the case of the $(p, 2pn)$ reaction [formation of ^{179}Hf^{m2} $(25/2^-)$] one of the outgoing protons excites the nucleus with successive neutron evaporation. In the $(p, 2p)$ reaction, on the contrary, both protons escape from the nucleus without interaction. The neutron evaporation rate depends on the excitation energy rather than on the incident proton energy. This explains the experimental results for production of ^{179}Hf^{m2} $(25/2^-)$ where the measured cross sections have a similar magnitude for all incident proton energies (Table II). The general magnitude of the cross section for the $(p, 2pn)$ reaction is higher than for the $(p, 2p)$ reaction since a larger fraction of nuclear matter may be involved in this process.

The $(p, \alpha\, n)$ reaction in formation of the highest spin isomer ^{177}Hf^{m2} $(37/2^-)$ demonstrates a similar energy dependence to the $(p, 2pn)$ reactions. This experimental result supports the suggestion that this process may more likely be interpreted by α particle emission rather than standard cascade $(p, 2p3n)$ mechanism. An additional argument is that it would be less probable to reach such a high-spin value by multiproton emission. The general magnitude of the cross section for knockout of an α particle is very low since it is difficult to find a preformed α cluster at the nuclear surface.

B. Isomer ratios

Isomer ratios (σ^m/σ^g) may be considered a measure of the probability for the formed nuclei to achieve the given high spin value. In order to calculate these values we used experimental σ^m and theoretically calculated σ^g values. To validate this approach and to check theoretical calculations, ground state cross sections for a broad variety of other isotopes have been experimentally measured.

In Table III some of the reliably determined experimental cross sections (mostly cumulative) for several isotopes of Lu, Hf, and W at 100, 145, 200, 350, and 500 MeV protons on the ^{181}Ta target are listed along with the corresponding calculated values. In Fig. 3 typical plots for calculated and mea-

TABLE IV. Isomer ratios σ^m(expt)/σ^g(theor) are given for σ^g(theor) calculated in the CEF model. The errors include experimental and theoretical uncertainties.

Isomer $(spin^\pi)$	Reaction	Proton energy (MeV)				
		100	145	200	350	500
^{178}Ta^m (7^-)	^{181}Ta$(p, p3n)$	0.37±0.19	0.37±0.19	0.38±0.19	0.40±0.20	0.37±0.19
^{180}Hf^m (8^-)	^{181}Ta$(p, 2p)$	0.011±0.006		0.024±0.012	0.030±0.015	0.033±0.017
^{177}Lu^m $(23/2^-)$	^{181}Ta$(p, \alpha p)$	0.023±0.012[a]		0.012±0.007	0.016±0.008	0.025±0.014
^{179}Hf^{m2} $(25/2^-)$	^{181}Ta$(p, 2pn)$	0.020±0.010		0.019±0.010	0.016±0.008	0.018±0.009
^{177}Hf^{m2} $(37/2^-)$	^{181}Ta$(p, \alpha n)$	0.0015±0.0008		<0.0034	0.0016±0.0008	0.0024±0.0013

[a]^{177}Lu is the only case when the ground state yield was measured experimentally; the value σ^m(expt)/σ^g(expt)=0.061±0.021. In the case of ALICE calculation σ^m(expt)/σ^g(theor)=0.14±0.07.

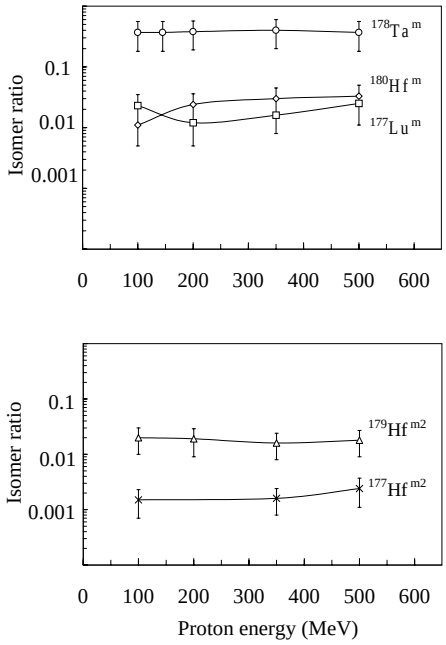

FIG. 4. Isomer ratio dependence on incident proton energy; (O), ^{178}Ta^{m}; (◇), ^{180}Hf^{m}; (□), ^{177}Lu^{m}; (△), ^{179}Hf^{m2}; (×), ^{177}Hf^{m2}.

sured ^{170}Hf and ^{169}Lu excitation functions for an incident proton of 100–580 MeV are also given. Cascade and hybrid models have been used for the calculations.

The nuclear reaction codes CEF (Cascade Evaporation Fission model) and HMS-ALICE were used in cascade and hybrid models correspondingly [12–15]. Both CEF and ALICE are in good agreement with the experimental results, but CEF provides a little better fit to the data for the given radionuclides in the most cases (Table III). Therefore, CEF calculated cross section values were used for determination of the isomer ratio. The real error bars for the isomer ratios may exceed 50% due to uncertainties in calculations (see Table IV) and experimental errors in isomer yield measurements. This however does not undermine our main interpretations and conclusions discussed below.

First, the general value of isomer ratios for high-spin isomeric states generated by intermediate-energy protons in these experiments were found to be small (Table IV). This differs considerably from the data given in Refs. [1–4] for interaction with pions.

Second, as one can see from Table IV and Fig. 4 the isomer ratio does not strongly depend on proton energy from 100 to 500 MeV. This clearly indicates that 100-MeV incident protons saturate the population of spin states for various isomers in our experiments (spins 7–37/2). The competition with the process of ground state formation does not depend strongly on the incident proton energy. But there is a competition with different reaction channels. This probably results in the cross section energy dependence in some cases discussed above.

Third, a clear tendency of isomer ratio decrease with the increase of the spin value (see Fig. 5) is observed. This is understandable since the probability of nuclear rotation to a higher-spin value should be lower. However, $(p, 2p)$ reaction (formation of the nuclei with spin value 8) is out of this trend: the isomer ratio is about 10–30 times lower than for spin value 7 induced in $(p, p3n)$ reaction. This may be because two emitted protons compensate each other partly resulting in a lower probability for residual nuclei with a high spin value. In the reaction $(p, 2pn)$ a higher-spin value 25/2 is excited easily since one of two emitted protons loses its energy to excite the core nucleus in the cascade process.

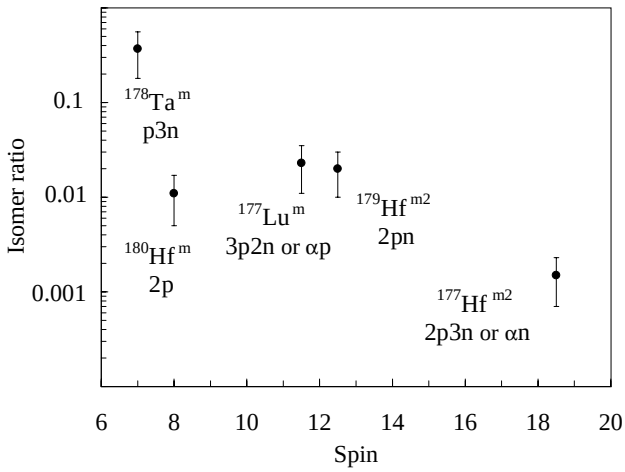

FIG. 5. Isomer ratio dependence on isomer spin at 100 MeV.

In this consideration it would be difficult to excite 37/2 spin value in the given $(p, 2p3n)$ reaction. So, the lower isomer ratio in this case seems reasonable. It is also possible that such a high-spin value is excited via emission of an α particle in the $(p, \alpha n)$ reaction. Therefore, it would be interesting to investigate the formation of the same isomer ^{177}Hf^{m2} $(37/2^{-})$ in a reaction with one-proton emission on enriched Hf targets. α-particle emission will be not possible in this case.

IV. CONCLUSION

A number of cross section and isomer ratio values are determined. The resulting angular momentum of the residual nuclei varies over a wide range. Based on experimental results, a qualitative explanation of the observed regularities is suggested. The proposed reaction mechanism may include the emission of clusters. A quantitative approach [19] with isomer yield calculation is desirable for a more rigorous explanation of the observed experimental data.

ACKNOWLEDGMENTS

We are thankful to M. Blann for many helpful theoretical discussions and for providing revised version HMS-ALICE code. The authors thank A. A. Razbash for recommendation in the development of radiochemical separation. The assistance of V. Yu. Gusev in the data analysis is greatly appreciated. This research work was supported in part by grants from the Russian Foundation for Fundamental Research and the National Research Council of Canada.

[1] V. S. Butsev *et al.*, JETP Lett. **21**, 181 (1975).
[2] H. S. Pruys *et al.*, Helv. Phys. Acta **50**, 199 (1977).
[3] C. J. Orth *et al.*, Phys. Rev. C **21**, 2524 (1980).
[4] V. S. Butsev, Izv. AN USSR **43**, 131 (1979).
[5] A. S. Iljinov, V. I. Nazaruk, and S. E. Chigrinov, Nucl. Phys. **A268**, 513 (1976).
[6] M. P. Locher and F. Myhrer, Helv. Phys. Acta **49**, 123 (1976).
[7] S. S. Gernstein, Sov. Phys. Usp. **124**, 455 (1978).
[8] O. F. Nemets and Yu. V. Hofman, *Handbook of Nuclear Physics* (Naukova Dumka, Kiev, 1975) (in Russian).
[9] A. S. Iljinov, V. G. Semenov, M. P. Semenova, N. M. Sobolevsky, and L. V. Udovenko, in *Production of Radionuclides at Intermediate Energies*, edited by H. Shopper, Landolt-Bornstein (Springer-Verlag, Berlin, 1991), Vol. 13a–d.
[10] U. Reus and W. Westmeier, At. Data Nucl. Data Tables **29**, 1 (1983); in *Table of Radioactive Isotopes*, edited by V. S. Shirley (LBL, Berkley, 1986).
[11] M. Cackette, *The GXL Gamma Spectrometry Code* (TRIUMF, Vancouver, 1996).
[12] A. S. Iljinov, M. V. Kazarnovsky, and E. Ya. Paryev, *Intermediate-Energy Nuclear Physics* (CRC Press, Boca Raton, FL, 1994), Chaps. 1 and 3.
[13] A. S. Iljinov *et al.*, Nucl. Phys. **A543**, 517 (1992).
[14] M. V. Mebel, A. S. Iljinov, C. Grandi, G. Reffo, and M. Blann, Nucl. Instrum. Methods Phys. Res. A **398**, 324 (1997); P. Hofmann *et al.*, Phys. Rev. C **49**, 2555 (1994).
[15] M. Blann, Phys. Rev. C **54**, 1341 (1996).
[16] V. P. Lunev, Yu. N. Shubin, C. Grandi, B. Poli, and A. Ventura, Nuovo Cimento Soc. Ital. Fis., C **A112**, 743 (1999); L. Milazzo-Colli and G. M. Braga-Marcazzan, Nucl. Phys. **A210**, 297 (1973).
[17] Y. Asano *et al.*, J. Phys. Soc. Jpn. **54**, 3734 (1985).
[18] B. Neidhart and K. Bachmann, J. Inorg. Nucl. Chem. **33**, 2751 (1971).
[19] M. Blann, M. B. Chadwick, and W. B. Wilson (unpublished).